Medical Image Processing and Numerical Simulation for Digital Hepatic Parenchymal Blood Flow

Marie-Ange Lebre[1], Khaled Arrouk[1], Anh-Khoa Võ Văn[1], Aurélie Leborgne[1], Manuel Grand-Brochier[1], Pierre Beaurepaire[1], Antoine Vacavant[1(✉)], Benoît Magnin[1,2], Armand Abergel[1,2], and Pascal Chabrot[1,2]

[1] Université Clermont Auvergne, SIGMA Clermont, CNRS, Institut Pascal, 63000 Clermont-Ferrand, France
antoine.vacavant@uca.fr
[2] Centre Hospitalo-Universitaire, 63003 Clermont-Ferrand, France

Abstract. This paper deals with the personalized simulation of blood flow within the liver parenchyma, by considering a complete pipeline of medical image segmentation, organ volume reconstruction, and numerical simulation of blood diffusion. To do so, we employ model-based segmentation algorithms developed with ITK/VTK librairies, CATIA software for volumetric reconstructions based on NURBS and Abaqus solution for adapted simulation of Darcy's law. After presenting experimental results of each step, we explore scientific and technical bottlenecks so that a valid digital hepatic blood flow phantom may be developed in our future research, in direct relation with current open challenges in this domain.

Keywords: Medical image analysis · Model-based segmentation · Liver · Blood flow simulation · 3D reconstruction · NURBS

1 Introduction

The liver has multiple key biological functions and is a very complex organ, from both anatomical and physiological considerations [13], as suggested by Fig. 1: the shape of the liver can vary considerably from one patient to another; its vascular system is composed of two blood inflows (red and purple in Fig. 1 and one outflow (blue in Fig. 1), contrary to other organs like kidney, brain composed of one of each, moreover portal vein, hepatic artery and hepatic vein are respectively then subdivided into complex tree-like networks; in the liver, each hepatic cell (hepatocyte) has a connection to those networks (and bile duct, green in Fig. 1) by sinusoids and possesses many functions: synthesize proteins, detoxify, secrete bile, *etc.*

The very complex tree-like networks finish with capillaries, also called sinusoids (less than 10 µm), which are invisible on images acquired from medical

S.A. Tsaftaris et al. (Eds.): SASHIMI 2017, LNCS 10557, pp. 99–108, 2017.
DOI: 10.1007/978-3-319-68127-6_11

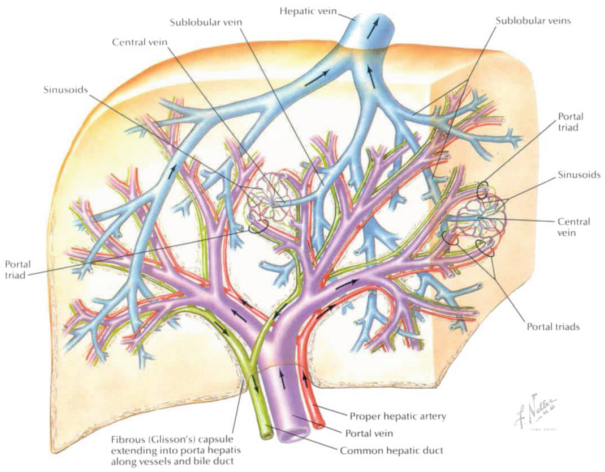

Fig. 1. Illustration of the complex vascular network of the liver with two input blood flows and one output. Image from [13] (Color figure online)

imaging systems such as MRI (Magnetic Resonance Imaging) or CT (Computed Tomography). Hence, simulating personalized blood transport and treatments (such as tumor embolization [12]) in an accurate way is a challenging question for the liver. Also, it would be a key to develop *in-silico* trials [21], to help medical doctors in defining embolization (transarterial chemo-embolization, radio-embolization, *etc.*) adapted to patients by using computer aided treatment planning, and to reduce animal experimentation for drug design and testing. The impact of such approach is high since liver cancer is the second leading cause of cancer-related death worldwide with 746,000 deaths in 2012 according to the World Health Organization (WHO) [22]. Therefore, numerous patients could benefit from these *in-silico* trials, by undergoing the best personalized treatments (as embolization) determined thanks to numerical testings.

In this paper, we present a complete pipeline devoted to simulate personalized blood flow within liver parenchyma (*i.e.* liver volume except vessels, thus comporting hepatic lobules). We also point out key scientific and technical problems of this process, and possible ways to solve them in future works. Another objective of this work is to draw the possible relations between image-based simulation and (model-based) medical image processing. The paper follows our pipeline and is organized as follows. Section 2 deals with the segmentation of liver volume and internal vessels, from CT and MRI volumes. Then, in Sect. 3, we explain how to obtain a valid 3D model appropriate for the simulation, which is exposed in Sect. 4. We finish by discussing this study and possible future works in Sect. 5.

2 Liver Segmentation in CT and MRI Modalities

Liver segmentation in MRI and CT is a challenging problem due to noise, low contrast and similar intensities with adjacent organs and tissues. Automatic liver segmentation is often performed in CT [3] but MRI provides more information for diagnosis purposes [1]. We have developed an automatic model-based method for both modalities. To do so, we first extract four statistical models with 68 livers segmented by clinical experts obtained from Shape2015 [10], IRCAD [14] and SLIVER07 [8] databases. The four models are constructed according to their variabilities (small to large) from a standard shape liver (mean dimensions of all volumes available in the datasets). Statistical model and all patient volumes have the same dimensions (voxel size: $1 \times 1 \times 1\,\mathrm{mm}^3$).

We first localize the liver on the images with the mean dimensions of a standard liver. This localization of the liver allows us to compute a threshold to isolate pixels that belong to the liver. After the thresholding on each slice, we apply a contour enhancement process. At this step we use the model the liver) as a probability map to localize the liver and we then perform an active contour segmentation method (fast marching) resulting in a binary mask. Finally, to erase errors due to over-segmentation by a process considering the global shape of the liver. Figure 2 illustrates results of the different steps.

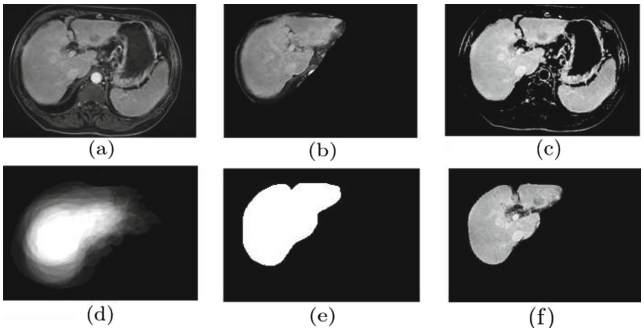

Fig. 2. Results of different step on MR images: (a) patient slice P_j with $j \in \{1, p\}$, (b) largest surface of the liver (threshold computation), (c) thresholding and contour enhancement, (d) liver model for localization and active contour method, (e) mask obtained, (f) segmentation result

In the second step, we extract the liver vessels within the 3D segmentation obtained previously from CT and MRI volumes. The contrast of the blood vessels in our images is quit good as a contrast agent injection is generally performed during the medical exam. Thus, we first tried a simple thresholding to segment the vascular network (see results in Fig. 3). Nonetheless, we also tried to apply two different vessel filters: the Sato vesselness based on the analysis of the Hessian matrix, which plays a role in a discriminating shape and orientation of tubular structures [16]; and the RORPO filter (Ranking the Orientation

Responses of Path Operators) [11], based on the notion of path operators from mathematical morphology. It allows a discrete, non linear and non local, 3D curvilinear structure analysis.

The automatic liver segmentation has been tested with 20 CT from the IRCAD database, 20 CT from the SLIVER07 challenge and 39 MR images from our radiology department. The ground truth of the liver segmentation is available for the SLIVER07 and IRCAD databases only, which permits us to calculate the mean Dice of our method, which is equal to $90,5\%$. The vessels extraction is tested on CT of the IRCAD database and MR images. Manual expert segmentations of the portal vein, the arterial vein and the venous system are available for the IRCAD database. The mean Dice is equivalent for the three vessels extraction methods, around 30%. The parameters are not yet optimized and more tests are needed, specially on MRI, but results are promising: Sato-filter is stable according to the different modalities but contains lot of noise, RORPO is promising for CT and results obtained with simple thresholding highly depend on patient's data. The entire process allows a 3D visualization of the patient liver with its vascular network, Fig. 3 illustrates results for two CT and one MRI volume.

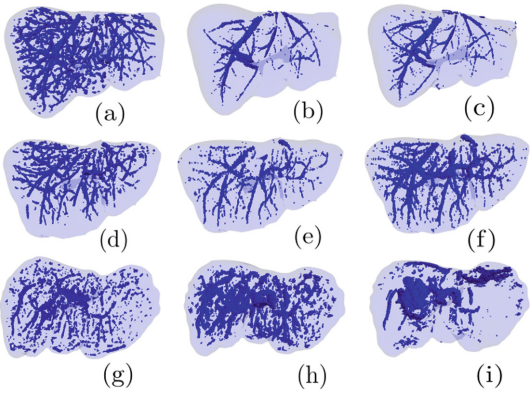

Fig. 3. Visualization of the liver segmentation (in light blue) and its vascular network (in dark blue). First two lines correspond to two CT and the third line corresponds to one MRI. Then (a), (d), (g) represent results with Sato filter, (b), (e), (h) results with the RORPO algorithm and (c), (f), (i) are calculated with a simple thresholding process (Color figure online)

3 Liver Components Reconstruction

In this work, the analysis is performed using a finite element (FE) solver. FE solver uses the geometric information provided by the 3D Computer-Aided Design (CAD) models. These 3D models can be a solid model or a surface model such as Non-Uniform Rational Basis Spline (NURBS, see *e.g.* [15]). Such models are not directly obtained from the CT, and therefore the NURBS model needs to be reconstructed in order to maintain the workflow required by the FE solver.

3.1 Liver Reconstruction

From the liver obtained by segmenting medical images (Sect. 2), we obtain a 3D triangular mesh by using the marching cubes algorithm, meaning that 3D points are spaced wrt. the segmented image resolution (*i.e.* the voxel size is $1 \times 1 \times 1\,\mathrm{mm}^3$). We also use a Laplacian smoothing operator to enhance the 3D mesh. To produce this mesh, we employ the Visualization Toolkit VTK, and export the reconstructed liver in the STL format (Stereolithography), as shown in Fig. 4a. We import the mesh into the CAD software CATIA®, which can be used to convert the 3D surface polygonal mesh into a NURBS surface model, as shown in Fig. 4b. This closed surface is subsequently filled to obtain a solid model needed to perform the FE analysis.

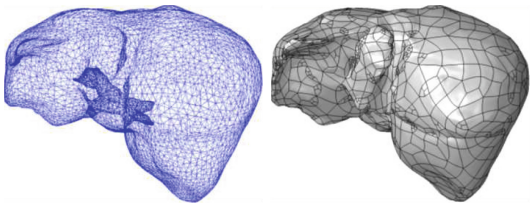

(a) (b)

Fig. 4. Reconstruction of the liver model: (a) Original surface mesh. (b) Volumetric CAD model. From an IRCAD sample [14]

3.2 Venous System Reconstruction

The model of the venous system is reconstructed from a surface polygonal triangular mesh (see Fig. 5a), but the procedure used for the liver cannot be directly applied. In fact, the preparation of a FE model for veins from a 3D CAD model is a difficult task, because the geometry of the veins is more complex, which may lead to distorted or non physical NURBS. The 3D surface model of the veins contains a large number of faces, some of which may be narrow or feature short edges that are smaller than the required FE size for 3D mesh generation. In our case, for instance, we frequently observed intersections between the opposite walls of a vein or NURBS with excessive curvature radii, which cannot be meshed by the FE software. Therefore, the radii of the veins have been slightly increased between 1–1.5 mm, in an adaptive way considering the mesh geometry by means of CATIA. The reconstructed and modified CAD model of the veins is shown in Fig. 5b. The hepatic artery is not included in this model, as it is considerably smaller than the vena cava and the hepatic vein, the input model used here did not include sufficient information.

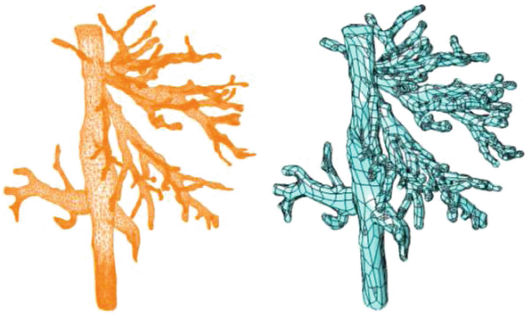

Fig. 5. Construction of the geometric vein model from an IRCAD example [14]: (a) Original surface mesh. (b) Volumetric CAD model

3.3 Boolean Operations

The geometry of the hepatic parenchyma HP is reconstructed from the previously described 3D CAD models (solid). Two Boolean subtractions are subsequently applied to remove the veins' volumes (portal veins PV and hepatic vein HV) from the liver's volume (LV), meaning that we calculate:

$$HP = (LV \setminus PV) \setminus HV. \tag{1}$$

An assembly model including all the reconstructed solids is prepared as shown in Fig. 6.

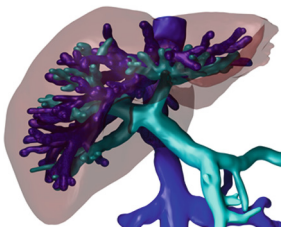

Fig. 6. Geometric model of the liver with the modified venous system (IRCAD sample [14])

4 Numerical Simulation of Blood Transport Within Liver Parenchyma

A porous medium model of the liver is developed in this paper. A similar approach at the microscopic scale is described in the literature [2,19]. The simulations are focused on the hepatic parenchyma and a 3-dimensional volume model

is implemented. Simulation of the flow of blood is possible using computational fluid dynamics (see *e.g.* [18,20]) but this approach is not considered here. The larger veins and arteries can be explicitly identified from the CT. They are subsequently excluded from the analysis and it is assumed that they can be replaced by appropriate boundary conditions. The smaller veins cannot be identified from the CT, as there are smaller than the resolution of the images. It is assumed as a simplifying hypothesis that all the unidentified veins and arteries behave as the parenchyma, and they are modeled with the properties of the porous medium.

4.1 Constitutive Equations

Darcy's law is used to model the flow of blood in the hepatic parenchyma; it is expressed as:

$$\mathbf{q} = \frac{k}{\mu} \nabla P, \tag{2}$$

where $\mathbf{q}$ denotes the flux of the fluid (expressed in volume of fluid per unit of surface and per unit of time, *i.e.* in m/s), ∇P denotes the gradient of the pressure of the fluid within the pores (liver lobules), k and μ are respectively the permeability of the bulk material and the viscosity of the fluid. The influence of gravity is neglected in Eq. 2, as we assumed that the difference of pressure in the portal vein and in the hepatic vein causes the blood flow; and that the volumetric forces have second order effects. The second constitutive equation is the conservation of the mass:

$$\nabla \cdot \mathbf{q} = 0, \tag{3}$$

where $\nabla \cdot$ is the divergence operator. It should be noted that the flux is not the actual velocity of the fluid, as it travels only in the pores and the solid material reduces the available space.

Equations 2 and 3 do not include any partial derivative of the fluid flux and pressure with respect to time as they describe the flow within the porous medium in steady state condition. This approximation allows us to reduce the numerical efforts associated with the analysis, and has been applied with success in the literature (see *e.g.* [2,19]). Homogeneous isotropic material properties are used for the hepatic parenchymal material, we have set $k = 1.56 \cdot 10^{-14}\,\mathrm{m}^2$ and the blood viscosity $\mu = 0.0024\,\mathrm{Pa.s}$.

The method is implemented in the commercial FE solver Abaqus. Darcy's law is available in this software, which is used by civil engineers to solve soil mechanics and hydraulics problems. 4-node tetrahedral elements are used, as they are versatile elements suitable for complex geometries. The model includes 585,219 elements and 110,266 nodes in total.

4.2 Boundary Conditions

The first boundary condition consists of applying no blood flux at the wall of the vein, nor at the surface of the liver, which is expressed as:

$$\mathbf{q} \cdot \mathbf{n} = 0 \tag{4}$$

at any point of a surface where this flux boundary condition is prescribed, **n** being the normal vector of the surface. This is the default boundary condition applied by the solver for all the free surfaces, excepted if another boundary condition is explicitly applied.

Specific boundary conditions are applied at the ends of the veins as they apply in the geometry reconstructed from the medical image. These veins are not included in the FE model, and their end surfaces are modeled as an inlet or as an outlet. Two modeling strategies are applicable; they consist of applying: (i) the fluid flux; (ii) the pressure of the fluid on the pores. The second strategy is used here as relevant information on the pressure in the hepatic and portal vein is available in the literature [19]. The pressure is 587 Pa at the ends of the portal veins and 200 Pa at the ends of the hepatic vein.

4.3 Experimental Results

Figure 7 shows the results of the FE analysis, the fluid pressure and flux are determined. It is observed that both quantities exhibit higher values in the vicinity of the veins end (as they are observed from the medical images).

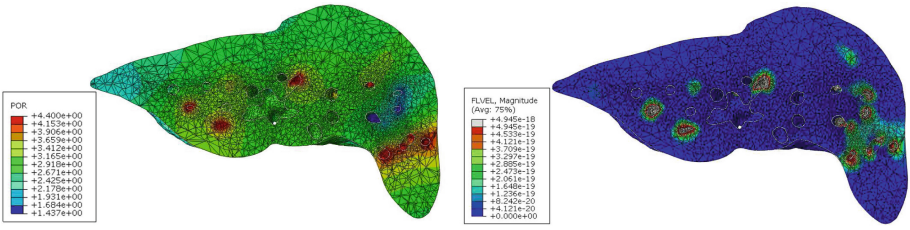

(a) (b)

Fig. 7. Results of the FE analysis (a) Fluid pressure in the parenchyma. (b) Blood flux

5 Discussion

In this paper, we have presented a complete pipeline dedicated to the simulation of blood flow within liver parenchyma from personal medical image data. We now propose to consider different technical and scientific issues, and possible solutions to be developed as future works.

Simulation outcome validation. As presented in Fig. 7, numerical simulation based on Darcy's law enables the computation of blood flow within liver parenchyma, by calculating flow pressure or velocity in each FE node of the 3D reconstructed object. To validate this process, we have to take into account the blood flow coming from liver vessels, by incorporating fluid dynamics. In this case, flow should be synchronized with cardiac rhythm, with the support of ECG signal for instance. To validate our digital blood flow, we could study the correlation with blood flow estimation from several image modalities (ultra-sound imaging, MR angiography, *etc.*) [4].

CT or other modalities only offer a coarse representation of liver vessels. A solution could be to reconstruct finer vessels by heuristics based on geometrical and anatomical features upon vascular shapes in this organ, as proposed by [17]. In Fig. 7, we can observe some parts of the liver with an abnormal flux and/or pressure (see left-most and bottom-right parts in particular) wrt. the rest of the organ. In reality, liver vascular network is organized so that every hepatic lobules participate in the treatment of blood. As a consequence, the vessels we have employed from IRCAD segmentation in this study do not have a sufficient precision to accomplish this task.

Also, simulation should also be driven by a multi-scale approach, so that we consider blood flow dynamics within hepatic lobules, like in [19]. This means that we should be able to draw the relation between possibly cirrhotic liver reconstructed from macroscopic images (CT, MRI) and microscopic data (histology).

Image processing quality and robustness. In our study, liver extraction method achieve an accuracy (Dice measure) of approximately 30% wrt. manual annotation provided by IRCAD dataset (see Fig. 3). And visual appreciation of results from MRI data suggest that the quality of vascular reconstruction would be even worst. From previous observations, we may suppose that simulation based on such reconstructions will suffer from a lower outcome quality compared to the one we have obtained with IRCAD segmentations in this paper. However, we have to be aware that image-based quality measurement is not forced to be correlated to simulation performance measurement. And if we consider *in-silico* trial as the final goal of our work, digital blood flow assessment should be the best way to judge the quality of previous segmentation tasks. This is also related to the current concern about evaluating the reproducibility and robustness of image processing tasks, by considering more applications [9].

Scalability, benchmarking and big data. In our pipeline, several operations have been produced by supervised manipulations: liver and vascular reconstruction, as exposed in Figs. 4 and 6 in CATIA, input/output labeling of vessels in Abaqus, *etc.* To be able to handle a large number of images (as our dataset of 39 MRI volumes, and even larger patient cohorts), automatic procedures should be developed. In this case, a first solution is to design home-made algorithms or use open-source solutions for volume reconstruction [6] and blood flow simulation [7]. Producing such automatic processes will also help in validating image processing tasks and the possible underlying models or atlases (as we propose in this article for the liver) for large amounts of data.

References

1. Bereciartua, A., et al.: Automatic 3D model-based method for liver segmentation in MRI based on active contours and total variation minimization. Biomed. Signal Process. Control **20**, 71–77 (2015)
2. Bonfiglio, A., et al.: Mathematical modeling of the circulation in the liver lobule. J. Biomech. Eng. **132**(11), 1–10 (2010)

3. Campadelli, P., et al.: Liver segmentation from computed tomography scans: a survey and a new algorithm. Artif. Intell. Med. **45**, 185–196 (2009)
4. Chow, P.K., et al.: The measurement of liver blood flow: a review of experimental and clinical methods. J. Surg. Res. **112**(1), 1–11 (2003)
5. El-Serag, H.B.: Hepatocellular carcinoma. New Engl. J. Med. **365**, 1118–1127 (2011)
6. Hang, S.: TetGen, a delaunay-based quality tetrahedral mesh generator. ACM Trans. Math. Softw. **41**(2), 11 (2015)
7. Hecht, F.: New development in FreeFem++. J. Numer. Math. **20**(3–4), 251–265 (2012)
8. Heimann, T., et al.: Comparison and evaluation of methods for liver segmentation from CT datasets. IEEE Trans. Med. Imaging **28**(8), 1251–1265 (2009)
9. Kerautret, B., Colom, M., Monasse, P. (eds.): RRPR 2016. LNCS, vol. 10214. Springer, Cham (2017)
10. Kistler, M., et al.: The virtual skeleton database: an open access repository for biomedical research and collaboration. J. Med. Internet Res. **15**(11), e245 (2013)
11. Merveille, O., et al.: Curvilinear structure analysis by ranking the orientation responses of path operators. IEEE Trans. Pattern Anal. Mach. Intell. **1** (2017). doi:10.1109/TPAMI.2017.2672972
12. Rammohan, E., et al.: Embolization of liver tumors: past, present and future. J. Radiol. **4**(9), 405–412 (2012)
13. Netter, F.H.: Atlas of Human Anatomy. Saunders, Philadelphia (2014)
14. Research Institute against Digestive Cancer. IRCAD dataset. http://www.ircad.fr/research/3d-ircadb-01/
15. Rogers, D.F.: An Introduction to NURBS. Morgan Kaufmann, San Francisco (2001)
16. Sato, Y., Nakajima, S., Atsumi, H., Koller, T., Gerig, G., Yoshida, S., Kikinis, R.: 3D multi-scale line filter for segmentation and visualization of curvilinear structures in medical images. In: Troccaz, J., Grimson, E., Mösges, R. (eds.) CVRMed/MRCAS -1997. LNCS, vol. 1205, pp. 213–222. Springer, Heidelberg (1997). doi:10.1007/BFb0029240
17. Schwen, L.O., Preusser, T.: Analysis and algorithmic generation of hepatic vascular systems. Int. J. Hepatol. **2012**, Article ID 357687 (2012)
18. Schwen, L.O., et al.: Spatio-temporal simulation of first pass drug perfusion in the liver. PLoS Comput. Biol. **10**(3), e1003499 (2014)
19. Siggers, J.H., et al.: Mathematical model of blood and interstitial flow and lymph production in the liver. Biomech. Model. Mechanobiol. **13**(2), 363–378 (2014)
20. Sousa, L.S., et al.: Finite element simulation of blood flow in a carotid artery bifurcation. In: Congress on Numerical Methods in Engineering, Coimbra (2011)
21. Viceconti, M., et al.: In silico clinical trials: how computer simulation will transform the biomedical industry. Avicenna-ISCT, Avicenna Project (2016)
22. World Health Organization: Liver cancer. Estimated incidence, mortality, prevalence worldwide in 2012. http://globocan.iarc.fr/old/FactSheets/cancers/liver-new.asp